Particulate matter resuspension from simulated urban green floors using a wind tunnel-mounted closed chamber

Inhye Seo[1], Chan-Ryul Park[2], Gayoung Yoo[1,3]

[1] Department of Applied Environmental Science, Kyung Hee University, Yongin, Republic of Korea
[2] Urban Forests Division, National Institute of Forest Services, Seoul, Republic of Korea
[3] Department of Environmental Science and Engineering, Kyung Hee University, Yongin, Republic of Korea

Corresponding Author:
Gayoung Yoo[1,3]
1732, Deogyeong-daero, Giheung-gu, Yongin, 17104, Republic of Korea
Email address: gayoo@khu.ac.kr

Abstract

Background. Green areas are thought to reduce particulate matter (PM) concentrations in urban environments. Plants are the key to PM reduction via various mechanisms, although most mechanisms do not lead to the complete removal of PM. Ultimately, PM falls into the soil via wind and rainfall. However, the fallen PM can re-entrain the atmosphere, which can affect plants capacity to reduce PM. In this study, we simulated an urban green floor and measured the resuspension of PM from the surface using a new experimental system, a wind tunnel-mounted closed chamber.

Methods. The developed system is capable of quantifying the resuspension rate at the millimeter scale, which is measured by using the 1 mm node chain. This is adequate for simulating in situ green floors, including fallen branches and leaves. This addressed limitations from previous studies which focused on micrometer-scale surfaces. In this study, the surfaces consisted of three types: bare sand soil, broadleaves, and coniferous leaves. The resuspended PM was measured using a light-scattering dust detector.

Results. The resuspension rate was highest of 14.45×10^{-4} s^{-1} on broad-leaved surfaces and lowest on coniferous surfaces of 5.35×10^{-4} s^{-1} ($p<0.05$) and was not proportional to the millimeter-scale surface roughness measured by the roller chain method. This might be due to the lower roughness density of the broad-leaved surface, which can cause more turbulence for PM resuspension. Moreover, the size distribution of the resuspended PM indicated that the particles tended to agglomerate at 2.5 μm after resuspension.

Conclusion. Our findings suggest that the management of fallen leaves on the urban green floor is important in controlling PM concentrations and that the coniferous floor is more effective than

40 the broadleaved floor in reducing PM resuspension. Future studies using the new system can be
41 expanded to derive PM management strategies by diversifying the PM types, surfaces, and
42 atmospheric conditions.
43

Introduction

45 Urban green spaces have been known to mitigate high atmospheric particulate matter (PM)
46 concentrations, and their PM mitigation effect has been reported by previous studies (Deng et al.,
47 2019; Heo and Bell, 2019; Jennings et al., 2021). Gómez-Moreno et al. (2019) and Cohen et al.
48 (2014) measured PM concentrations at different distances from urban parks in Madrid (Spain)
49 and Tel-Aviv (Israel), and they observed a lower concentration inside the park than outside, with
50 a degree of 50% and 70% respectively. Yoo et al. (2020) measured the extent of PM reduction
51 by passing through the urban park in Sihwa (Korea), and the reduction rates were up to 56.4%.
52 Further, a number of researchers have reported that PM reduction occurs even in narrow green
53 spaces, such as vegetation barriers in urban streets (Chen et al., 2021; He et al., 2020; Kończak et
54 al., 2020; Mori et al., 2018).
55 The main mechanisms of PM reduction by plants are adsorption and absorption (Shi et al., 2017;
56 Wang et al., 2019). While adsorption is the physical contact of PM with the plant surfaces such
57 as trichomes, epicuticular wax, and bark, the absorption mechanism involves the entrance of PM
58 to the stomata and cuticles (Escobedo & Nowak, 2009; L. Chen et al., 2017; Ha et al., 2021).
59 When PM is absorbed through the plant's stomata it is converted to less or non-toxic matter and
60 stored in the vacuole or cell wall. This is the exhaustive removal process of PM although the
61 amount is minor (McDonald et al., 2007; Wróblewska and Jeong, 2021). However, most PM is
62 deposited and adsorbed on the vegetation surface and they enter the litter and soil layers or re-
63 entrain into the atmosphere (Cai et al., 2019; Diener and Mudu, 2021; Henry, 2018; Xu et al.,
64 2020). This is called PM resuspension, which is the mechanism by which PM deposited on
65 vegetation and soil surfaces is removed from the surface by external factors such as wind and
66 surface vibration and re-entrained back into the airflow (McPherson et al., 1998; Ould-dada &
67 Baghini, 2001; Henry & Minier, 2014).
68 Generally, PM resuspension is described as a function of the adhesion forces between the
69 particle, the surface, and the fluid friction velocity (Loosmore, 2003; Nasr et al., 2019). The
70 surface roughness is regarded as one of the most influential variables affecting PM resuspension
71 because it has a significant impact on the adhesion forces on multi-scales (Qian et al., 2014). The
72 largest scale of surface roughness that can affect PM resuspension could be the macrostructure of
73 urban areas, such as buildings and tree canopies, and there are smaller surface roughness scales
74 contributed by the shrubs/grass level (Salizzoni et al., 2008; Nasr et al., 2020). However, most of
75 the studies have been conducted on microscale surface roughness such as leaf morphology using
76 a single leaf (Speak et al., 2012; H. Wang et al., 2015; L. Chen et al., 2017; Xu et al., 2020).
77 These studies focused on investigating the effect of leaf microstructure or chemical traits on PM
78 resuspension and reported that the high roughness of leaf adaxial and abaxial surfaces
79 contributed to PM capture (Zhang et al., 2017; Zhao et al., 2019).

80   Our question was whether these microscale properties of surface roughness of a single leaf could
81   explain the effect of urban green floor on PM resuspension (Amato et al., 2013; Han et al.,
82   2020). When focusing on the role of urban greenery in PM reduction, the scale to be noted
83   should be expanded to a larger structure consisting of fallen branches, roots, leaves, and soil. At
84   this scale, the physical structure of litter layer create boundary layer to make turbulence and the
85   high surface roughness could lead to rather higher PM resuspension (Krogstad and Antonia,
86   1999; Volino et al., 2009; Wu et al., 1992). Despite of this complicated scale matter in PM
87   resuspension, it is hard to find the studies on PM resuspension at the green floor level.
88   One of the main reasons why there are few previous studies simulating the effect of different
89   urban green floor conditions on PM resuspension could be the absence of a proper experimental
90   setup at this scale. The existing PM resuspension experiment settings are usually equipped with
91   sophisticated controls over environmental conditions and contamination (Kim et al., 2016;
92   Kottapalli and Novosselov, 2021; Li et al., 2022). As these experiments focus on the specific
93   traits of the surface affecting resuspension, the scale of target surface is generally small
94   (microscopic, nanoscopic) and only the pure surface materials were used. This small scale
95   experimental setup is definitely not suitable for investigating the effects of green floor where the
96   diverse litters and soil are mixed. Therefore, it is necessary to develop the proper experimental
97   settings at the litter layer scale, which can function as the bridge between microscale pure surface
98   experiment and in situ measurement of PM resuspension.
99   Using the developed experimental system, we examined the difference in PM resuspension rates
100   by the urban green floor types with different surfaces, composed of bare soil, bare
101   soil+coniferous litter, and bare soil+broadleaf litter. The working hypotheses were as follows:
102   1) PM resuspension would be lower in the presence of litter layers compared to the bare soil
103   due to higher surface roughness.
104   2) PM resuspension would be different depending on whether it is a single leaf or a layer of
105   leaves.
106

107   **Materials & Methods**

108   *2.1 Resuspension chamber system design*

109   We developed an acrylic chamber system (810 × 810 × 1400 mm (L×W×H); Fig. 1) comprising
110   a wind tunnel and a measurement chamber surrounding the tunnel. The wind tunnel has an inlet
111   of PM (⌀ 10 mm) on the top and a target surface frame (300 × 100 mm (L×W), 3 mm thick) on
112   the bottom, where various types of surfaces can be placed. Detachable sliding doors are installed
113   on both sides of the wind tunnel and a circulation fan (⌀ 80 mm) is in the center of the top side
114   for scattering PM. The wind tunnel was mounted on a frame in the middle of the measurement
115   chamber, and the main fan was placed on one side of the frame. The main fan was connected to
116   an external controller that controlled the wind speed. The controller was programmed to set the
117   wind speed at the desired intensity and duration up to 15 m·s^{-1} in units of 1 m·s^{-1}.

118 The measurement chamber has a rubber-packed door in front, where the wind tunnel slides
119 horizontally. At each apex of the chamber, fans (⌀ 80 mm) were mounted for the internal
120 circulation. To prevent experimental errors, antistatic films were attached to all the acrylic
121 surfaces.
122 To verify whether the chamber system operated with the intended design, a verification
123 experiment was conducted. The experiment aimed to verify the following: 1) the air only escapes
124 through the outlet connected to the detecting sensor and not through the seams or door of the
125 chamber; and 2) the air flow generated by the main fan and the mixing fans is well distributed
126 throughout the chamber. To observe the air flow in the chamber, dry ice was placed in the center
127 of the wind tunnel, and the sublimated gas from the dry ice was visualized by video.
128 As we intended to detect the total amount of PM scattered in the wind tunnel and that floating in
129 the chamber, we connected the measurement device through the bottom hole (air outlet), and the
130 device detected the PM concentrations by pumping air through the tubing. The measurement
131 device was EDM 164 (GRIMM, Germany), which is a light-scattering dust detector that is
132 widely used to measure atmospheric PM concentrations (Dahari et al., 2020; Münch et al., 2020;
133 Kabelitz et al., 2021). Table 1 presents the performance evaluation results and details of EDM
134 164.

135 *2.2 PM resuspension experimental design*

136 *2.2.1 Particulate matter sample*

137 Standard reference material (SRM) No. 2786 of the National Institute of Standards &
138 Technology (NIST) was used as the PM sample. SRM components included polycyclic aromatic
139 hydrocarbons (PAHs), nitro-substituted PAHs, sugars, inorganic constituents and other natural
140 atmospheric substances. This was in line with our experimental purpose of simulating the
141 resuspension of atmospheric pollutants.
142 Information on the mass fractions and particle size distribution of the sample was provided by
143 NIST and were measured using laser diffraction instruments (Mastersizer 2000, Malvern
144 Panalytical Ltd, UK; Table 2). The diameter of all the particles was less than 20 μm, and the
145 mean particle diameter of the sample was less than 4 μm.

146 *2.2.2 Target surface preparation*

147 To simulate resuspension from different urban green floors, the target surfaces were prepared in
148 three types: sand only, sand with broadleaf litter, and sand with coniferous litter. The sand-only
149 surface consisted of a soil layer with a depth of 10 mm, and the other two surfaces consisted of a
150 10 mm soil layer and a litter layer (Fig. 2). The soil layer was composed of river sand to simulate
151 the soil texture of urban soil (Jim & Ng, 2018; Caplan et al., 2019; Romzaykina et al., 2021).
152 Fallen leaves were collected from an urban forest located in Suwon, Gyeonggi-do, Korea, and
153 separated into broad and coniferous leaves. The species of the collected leaves were *Quercus*
154 *mongolica*, *Robinia pseudoacacia*, and *Quercus acutissima* for broadleaves, and *Pinus densiflora*

155 for coniferous leaves, which are commonly found in temperate forests. All materials were
156 washed under running water and dried at 105 °C for more than 6 h.

157 *2.2.3 Experimental condition and chamber operation*

158 A preliminary experiment was conducted to determine the optimal wind speed for the
159 experiment and the amount of PM to be injected. Although all the soil and leaves were cleaned
160 before the experiment to prevent PM suspension from the soil and leaves themselves, the
161 background suspension from surface materials needed to be determined to eliminate data
162 contamination. Thus, we ran the wind tunnel with different surfaces installed (four replications)
163 without adding SRM 2786 and applied wind speeds of 1, 2, and 4 $m·s^{-1}$, which were in the range
164 of the wind profile in the urban area; thus, the background suspension rate was identified
165 (Memon et al., 2010; Chow et al., 2016). The results showed that significant differences in the
166 amount of PM suspended by different surface types were evident only when the wind speed was
167 4 $m·s^{-1}$. Hence, we regarded a wind speed of 4 $m·s^{-1}$ as the optimum condition to differentiate the
168 effect of the surfaces on the suspension. We also found that the average amount of background
169 suspension was 5 mg per surface with 8 mg of maximum for all types of surfaces. Therefore, 9
170 mg of SRM material per surface was added, which is a sufficient amount of PM input to
171 differentiate the signal from the background noise.
172 To reduce errors caused by environmental conditions, the air temperature and relative humidity
173 of the chamber were continuously monitored using a digital climate measuring instrument
174 (Model 480, Testo AG, DE). The temperature and relative humidity inside of the chamber were
175 maintained at 20.75–22.14 ℃ and 58.85–63.70%, respectively.
176 To deposit PM on each surface, a wind tunnel was closed with sliding doors on both sides, and
177 PM was introduced into the top injection port of the tunnel (Fig. 1). The injected PM was
178 dispersed by running the fan for 30 min and allowed to settle for at least one day (Qian et al.,
179 2008). After the deposition was completed, the sliding doors were removed from both ends of
180 the wind tunnel and immediately mounted on the frame inside the chamber. After the wind
181 tunnel was mounted on the frame, the door of the chamber was closed and the concentration of
182 PM inside the chamber was monitored. We stabilized PM using a small air purifier (CADR
183 13$m^3·h^{-1}$, Model AP130MWKA, LG Electronics, KR) until the PM concentration in the chamber
184 reached zero. The stabilizing procedure eliminated the influence of the external PM flowing into
185 the chamber when the wind tunnel was mounted. If the PM concentration was kept low, the air
186 purifier was stopped, and the main fan was operated for 10 min to resuspend the PM deposited
187 on the target surface (Braaten et al., 1990). We expected that once the main fan was on, the PM
188 on the surface would be resuspended and blown on both sides of the wind tunnel. The suspended
189 PM circulated inside the chamber and was finally collected through the hole at the bottom of the
190 chamber connected with EDM 164. Fig. 3 shows that the internal PM concentration increased
191 due to resuspension of the PM when wind was applied; when the wind stopped, the concentration
192 started to decrease and converged on zero over time. The time spent for each experimental run

193   varied from 40 to 200 min, depending on how fast the PM settled. All experiments were repeated
194   four times.

195   *2.3 Measurements*

196   *2.3.1 Surface roughness*

197   The roughness of the three surface types was measured using the roller chain method (Saleh,
198   1993). This method is easy, cost-efficient, and is widely used in field investigations (Gilley and
199   Kottwitz, 1996; Jester and Klik, 2005; Thomsen et al., 2015). To measure the surface roughness
200   in millimeters, a roller chain with a node length of 1 mm and a total length of 30 cm was used.
201   The roller chain was placed diagonally on the target surface, and the length of the Euclidean
202   distance between the two ends of the chain was measured. The measurements were conducted
203   three times before scattering the PM on the surface. The result of the measurement was derived
204   from the chain roughness (Cr) index and was determined using the following equation (Saleh,
205   1993):
206    $Cr = (1 - L_2/L_1) \times 100$ (1)
207   where L_1 is the distance over the surface [m] and L_2 is the Euclidean distance [m].
208   To validate the roller chain method, we used stereo photograph image analysis, which is
209   frequently used to measure soil surface roughness (Jester and Klik, 2005; Thomsen et al., 2015).
210   The target surface was photographed at two points with the same height of 80 cm using a digital
211   camera (D850, Nikon) with a 30 mm lens. The collected photographs were analyzed using
212   ImageJ software (Schneider et al., 2012) and the roughness calculation plugin (Chinga et al.,
213   2007). To compare the two indices, both were normalized by scaling to a range. Using the plot
214   profile function of ImageJ, we also calculated the roughness density (Λ) which is described as
215   the following equation (MacDonald et al., 2016):
216    $\Lambda = \Sigma k_n / \lambda$ (2)
217   where k_n is the roughness height of each projection, and λ is the length of the surface without
218   projections. The roughness density stands for the degree to which roughness projections are
219   distributed per unit area or section.

220   *2.3.2 PM resuspension*

221   The concentration and particle size distribution of the resuspended PM were continuously
222   measured at 6 s intervals using an EDM 164 placed at the bottom of the chamber. The amount
223   and rate of resuspended PM were derived using the following equations:
224    $Re_M(mg) = \Sigma_0^t C_n \times Q \times t_e$ (3)
225    $Re_R(s^{-1}) = Re_M/(M_i \times t_e)$ (4)
226   where Re_M is the amount of resuspended PM [mg], t is the time taken from the start of the
227   experiment until the concentration of PM in the chamber reaches zero [min], C is the
228   concentration of PM in the chamber [$\mu g \cdot m^{-3}$], Q is the inflow rate [$L \cdot min^{-1}$], t_e is the operating

229   time of the main fan [min], Re_R is the rate of resuspended PM [s^{-1}], and M_i is the initial input
230   amount of PM [mg].
231   The particle size distribution of the resuspended PM sample was compared to that of the original
232   PM sample. We modified the particle size distribution data provided by NIST using atmospheric
233   particle density data and used it as the distribution of the original PM sample (S. Kim et al.,
234   2008). The total number of resuspended particles was collected by the detector and averaged by
235   surface type.

236   *2.4 Data analysis*

237   Statistical analysis was conducted using the R software (version 4.1.1). Normal distribution of
238   the data groups was performed using the Kolmogorov–Smirnov normality test with ks.test
239   function, and homogeneity of variances was checked using bartlett.test function. Statistical
240   significance was tested using analysis of variance (one-way ANOVA) test. The results were
241   visualized and schematized using ggplot2 library in R and SigmaPlot software (version 12.5).
242

243   **Results and Discussion**

244   *3.1 Experimental design verification*

245   We found that the sublimating gas from the dry ice did not leak through the seams or door of the
246   chamber (Fig. 4). The air moved out of the wind tunnel by the horizontal flow generated by the
247   main fan and was circulated to the entire chamber by the mixing fans. Air outflow was only
248   found in the bottom hole of the chamber, which was connected to the detector. This indicates that
249   our system can detect the entire amount of PM resuspended from the surface at the scale of
250   simulating the urban green floor, thus the PM resuspension rate can be quantified.
251   Our system has advantages over existing experimental setups in two ways. First, it overcomes
252   the size limitation. A number of existing studies have used a small target surface (usually < 100
253   cm^2) because their research objectives focused on the effects of the physical and chemical
254   characteristics of pure materials on resuspension (Kim et al., 2016; Kottapalli and Novosselov,
255   2021; Li et al., 2022). This small surface area makes it possible to correctly quantify the total
256   number of resuspended particles within the system by counting the number of particles
257   remaining on the surface before and after resuspension. However, to simulate surfaces such as
258   urban green floors, roadsides, and agricultural fields, a larger surface size is required, which
259   makes it impossible to use counting methods to quantify the resuspension rate (Qian & Ferro,
260   2008; Martuzevicius et al., 2011; Maffia et al., 2021). Our system overcame this limitation
261   because the size was large enough to simulate urban greens, and the closed system was able to
262   capture all the particles resuspended within the system and accurately quantify them.
263   The second advantage is the versatility of wind tunnels, which enables the use of diverse
264   surfaces. Because of this structure, we can simulate various types of surfaces and conduct
265   replicated experiments with less preparation work, such as cleaning and stabilizing. This

266   versatility of the system implies that it can be used to investigate any interactions between the
267   atmosphere and soil ecosystem.
268   In summary, the system we developed was large enough to simulate the urban green floor
269   composed of soil and diverse leaves, and cost-effective but able to accurately quantify the total
270   amount of PM resuspension within the system.

271   *3.2 Surface roughness and PM resuspension*

272   The Cr index was significantly different among different surface types (Fig. 5, $p<0.001$). It was
273   highest on the broadleaf surface, with an average of 10.69 ($\pm$ 0.41), followed by the conifer and
274   sand surfaces. The results of the surface roughness analysis using Image J software were
275   consistent with those from the roller chain method. The Pearson correlation coefficient between
276   the two was 0.87 ($p<0.005$). These results indicate that the broadleaves created a much more
277   uneven floor than the conifers and sand did at the millimeter scale.
278   The resuspension rates were 14.45×10^{-4} s^{-1} ($\pm$ 4.97×10^{-4}), 5.35×10^{-4} s^{-1} ($\pm$ 4.04×10^{-4}), 7.34×10^{-4}
279   s^{-1} ($\pm$ 3.31×10^{-4}), on broadleaf, conifer, and sand surfaces, respectively (Fig. 6). Our resuspension
280   rates were within the range of the other PM resuspension experiments conducted using various
281   methods, which implies that our design was robust enough to produce reliable results (Krauter
282   and Biermann, 2007; Kim et al., 2016). The resuspension rate of the broadleaf surface was
283   significantly higher than that of the other two surfaces ($p<0.05$). These results are inconsistent
284   with our first hypothesis, as well as other existing studies that reported a negative correlation
285   between surface roughness and PM resuspension on a micro-scale (Kearns and Bärlocher, 2008;
286   Liang et al., 2016; Zhang et al., 2020, 2022). Leaf hairs, which make the surface uneven, were
287   reported to increase the surface area to intercept PM and make it harder for PM to get off the
288   leaves (Zheng and Li, 2019). Moreover, there was a greater chance for PM retention on the leaf
289   surface when the size of the PM was similar to the surface roughness (Nasr et al., 2019). This
290   inconsistency well represented the importance of roughness scales. Our result indicated that high
291   surface roughness at the litter layer scale could rather increase PM resuspension, the opposite
292   trend with the microscopic scale.
293   The effects of whether a single leaf or layer of leaves on resuspension was also different when
294   we compared our results with those from Kim et al. (2022), which supported our second
295   hypothesis. Kim et al. (2022) reported that a single leaf of broadleaved species with a larger
296   specific leaf area (SLA) or length of margin per leaf area (ML) captured more PM than
297   coniferous leaves. This is contrasted with our result that the layer of broadleaves had a higher
298   resuspension rate. This might be due to the higher turbulence in the array of broadleaves, where
299   erratic flutter and a rugged boundary layer were created. This could not be observed in the
300   experiment using a single leaf (Nicholson, 1993; Henry & Minier, 2014; X. Zhang et al., 2020).
301   The contrasting pattern of the effect of surface roughness on resuspension could be related to the
302   turbulence energy varying on different scales. This was explained by the concept of roughness
303   density (Sigal & Danberg, 1990; MacDonald et al., 2016). Roughness density was defined as the
304   distance-to-height ratio in the transverse plane of the target surface. Turbulent energy decreased

305   with increasing roughness density up to a threshold value, beyond which it showed the opposite
306   trend. Following this idea of roughness density and turbulence energy, we suggested a possible
307   conceptual diagram about the relationship between the PM resuspension rate and the surface
308   roughness density by its scale (Fig. 7). On the micrometer scale, negative correlation between
309   PM resuspension and surface roughness was found from the results of previous studies (Li et al.,
310   2022; Zheng and Li, 2019). On the millimeter scale, our data showed that there was a positive
311   relationship between resuspension rate and surface roughness density (r = 0.4654, p<0.001). The
312   roughness density of the broadleaf surface (3.82 ± 0.20) was greater than that of the coniferous
313   surface (1.30 ± 0.08) and both values exceed the threshold value (0.18) suggested by MacDonald
314   et al. (2016). This indicates that the surface roughness index must include roughness density
315   information to predict PM resuspension at any scale.

316

317   *3.3 The change of resuspended PM size distribution*

318   The number of resuspended particles showed trends similar to the total resuspension rates (Fig.
319   8). The resuspended PM number was highest on the broadleaf layer in less than 0.5 μm and
320   lowest on the coniferous layer through all size ranges. The initial particles have the highest
321   number in particle diameter of 0.4 μm.
322   The size distribution of initial particles showed that most of the particles were smaller than 1 μm.
323   Interestingly, the size distribution of resuspended PM had a new peak in the range of 1.5–3 μm,
324   which was not observed in the initial input sample. The result of peak formation in the range of
325   1.5–3 μm on all the surfaces suggests that the small particles gradually aggregated, without
326   permanently maintaining their original particle size. Our argument was supported by several
327   studies (Fan et al., 2019; Yin et al., 2020). Fan et al. (2019) simulated the PM size enlargement
328   by heterogeneous condensation using numerical model and found the PM smaller than 0.2 μm
329   was condensed to reach at 5 μm. Similarly, Yin et al. (2020) observed particle coagulation on a
330   single leaf surface and reported that the average size of particles grew from 0.48 μm to 3.40 μm.
331   The factors influencing particle coagulation were suggested as initial particle, humidity, wind,
332   temperature and residence time (Fan et al., 2019; Kim et al., 2016; Wu et al., 1992; Yin et al.,
333   2020). Physiological activity such as transpiration was also reported to affect the coagulation of
334   particles by thermal diffusion (Ryu et al., 2019; Yin et al., 2020). In our experiment, we
335   speculated that wind collision was the most probable factor for coagulation because the constant
336   wind at 4 m/s was blown throughout the experiment which must have generated turbulent flow
337   (Herner et al., 2006). The effect of humidity on coagulation also explained our results because
338   we maintained the relative humidity as relatively high (58 – 63%). As we used the dried leaves,
339   the effect of leaves' physiological activity might have been minimal. Our data on the size
340   redistribution after resuspension indicated that the mean size of resuspended particles was larger
341   than the originally deposited particles. Our size distribution data implied the role of urban green
342   floors in enlarging the particle sizes, which can make PM easier to re-deposit.

343

Conclusions

This study simulated the resuspension of PM from urban green floors by developing a new experimental design. Our newly developed chamber is cost-effective, accurate, and versatile for quantifying PM resuspension from diverse simulated urban green floors, overcoming the limitations of the existing resuspension experimental setup. The usability of this chamber is not limited to resuspension experiments and can be expanded to experiments investigating the interaction between the atmosphere and any surface with diverse materials.

Our results showed the significantly lower resuspension rate on the coniferous surface than on the other surfaces. This indicated the importance of the selection of plant species when designing the urban green areas for the PM mitigation. The fact that coniferous trees, which are known to be effective in capturing PM, were also good at preventing resuspension, supports the current management practice of planting more coniferous trees in urban greens.

As the effect of surface roughness on PM resuspension is significant both on the micro- and millimeter scales, the roughness scale should be noted when interpreting the results. We adopted the concept of roughness density for explaining the different effects of roughness on multi-scales. The roughness density had a positive correlation with the resuspension rate (p<0.001) on the millimeter scale. Our results emphasized the need for PM resuspension study under the condition closer to the real situation. The size distribution of resuspended particles showed a new and larger peak around 1.5-3 μm, suggesting coagulation which makes the role of urban green floor even more promising in terms of PM mitigation.

The relationship between roughness density and resuspension rate in our study could be used as input parameters for atmospheric models for simulating PM dynamics. In addition, our implications could provide an insight when interpreting continuous PM monitoring time series data. By diversifying the surface materials and air particulate pollutants, our experimental setup would provide affluent data for model improvement and help identify the important factors influencing PM resuspension.

Acknowledgements

We appreciate Minseop Jeong, Wanseop Jeong and Seok-yeong Jeong, who sincerely helped with the experimental procedures.

References

Amato, F., Schaap, M., Gon, H.A.C.D. van der, Pandolfi, M., Alastuey, A., Keuken, M., Querol, X., 2013. Short-term variability of mineral dust, metals and carbon emission from road dust resuspension. Atmos. Environ. 74, 134–140.

Braaten, D.A., Paw U, K.T., Shaw, R.H., 1990. Particle resuspension in a turbulent boundary layer-observed and modeled. J. Aerosol Sci. 21, 613–628.

Cai, M., Xin, Z., Yu, X., 2019. Particulate matter transported from urban greening plants during precipitation events in Beijing, China. Environ. Pollut. 252, 1648–1658.

383   Caplan, J.S., Galanti, R.C., Olshevski, S., Eisenman, S.W., 2019. Water relations of street trees
384   in green infrastructure tree trench systems. Urban For. Urban Green. 41, 170–178.
385   Chen, L., Liu, C., Zhang, L., Zou, R., Zhang, Z., 2017. Variation in Tree Species Ability to
386   Capture and Retain Airborne Fine Particulate Matter(PM2.5). Sci. Rep. 7, 1–11.
387   Chen, X., Wang, X., Wu, X., Guo, J., Zhou, Z., 2021. Influence of roadside vegetation barriers
388   on air quality inside urban street canyons. Urban For. Urban Green. 63, 127219.
389   Chinga, G., Johnsen, P.O., Dougherty, R., Berli, E.L., Walter, J., 2007. Quantification of the 3D
390   microstructure of SC surfaces. J. Microsc. 227, 254–265.
391   Chow, W.T.L., Akbar, S.N.A.B.A., Heng, S.L., Roth, M., 2016. Assessment of measured and
392   perceived microclimates within a tropical urban forest. Urban For. Urban Green. 16, 62–75.
393   Cohen, P., Potchter, O., Schnell, I., 2014. The impact of an urban park on air pollution and noise
394   levels in the Mediterranean city of Tel-Aviv, Israel. Environ. Pollut. 195, 73–83.
395   Dahari, N., Latif, M.T., Muda, K., Hussein, N., 2020. Influence of meteorological variables on
396   suburban atmospheric PM2.5 in the southern region of peninsular Malaysia. Aerosol Air
397   Qual. Res. 20, 14–25.
398   Deng, S., Ma, J., Zhang, L., Jia, Z., Ma, L., 2019. Microclimate simulation and model
399   optimization of the effect of roadway green space on atmospheric particulate matter.
400   Environ. Pollut. 246, 932–944.
401   Diener, A., Mudu, P., 2021. How can vegetation protect us from air pollution? A critical review
402   on green spaces' mitigation abilities for air-borne particles from a public health perspective
403   - with implications for urban planning. Sci. Total Environ. 796, 148605.
404   Escobedo, F.J., Nowak, D.J., 2009. Spatial heterogeneity and air pollution removal by an urban
405   forest. Landsc. Urban Plan. 90, 102–110.
406   Fan, F., Zhang, S., Wang, W., Yan, J., Su, M., 2019. Numerical investigation of PM2.5 size
407   enlargement by heterogeneous condensation for particulate abatement. Process Saf.
408   Environ. Prot. 125, 197–206.
409   Gilley, J.E., Kottwitz, E.R., 1996. Random roughness assessment by the pin and chain method.
410   Appl. Eng. Agric. 12, 39–43.
411   Gómez-Moreno, F.J., Artíñano, B., Ramiro, E.D., Barreiro, M., Núñez, L., Coz, E.,
412   Dimitroulopoulou, C., Vardoulakis, S., Yagüe, C., Maqueda, G., Sastre, M., Román-
413   Cascón, C., Santamaría, J.M., Borge, R., 2019. Urban vegetation and particle air pollution:
414   Experimental campaigns in a traffic hotspot. Environ. Pollut. 247, 195–205.
415   Ha, N., Seo, E., Kim, S., Lee, S.J., 2021. Adsorption of nanoparticles suspended in a drop on a
416   leaf surface of Perilla frutescens and their infiltration through stomatal pathway. Sci. Rep.
417   11, 1–13.
418   Han, D., Shen, H., Duan, W., Chen, L., 2020. A review on particulate matter removal capacity
419   by urban forests at different scales. Urban For. Urban Green. 48, 126565.
420   He, C., Qiu, K., Pott, R., 2020. Reduction of traffic-related particulate matter by roadside plants:
421   effect of traffic pressure and sampling height. Int. J. Phytoremediation 22, 184–200.
422   Henry, C., 2018. Particle resuspension from complex surfaces: current knowledge and
423   limitations.
424   Henry, C., Minier, J., 2014. Progress in particle resuspension from rough surfaces by turbulent fl
425   ows. Prog. Energy Combust. Sci. 45, 1–53.
426   Heo, S., Bell, M.L., 2019. The influence of green space on the short-term effects of particulate
427   matter on hospitalization in the U.S. for 2000–2013. Environ. Res. 174, 61–68.

428   Herner, J., Ying, Q., Aw, J., Gao, O., Chang, D., Kleeman, M., 2006. Dominant mechanisms that
429   shape the airborne particle size and composition distribution in Central California. Aerosol
430   Sci. Technol. 40, 827–844.
431   Jennings, V., Reid, C.E., Fuller, C.H., 2021. Green infrastructure can limit but not solve air
432   pollution injustice. Nat. Commun. 12, 10–13.
433   Jester, W., Klik, A., 2005. Soil surface roughness measurement - Methods, applicability, and
434   surface representation. Catena 64, 174–192.
435   Jim, C.Y., Ng, Y.Y., 2018. Porosity of roadside soil as indicator of edaphic quality for tree
436   planting. Ecol. Eng. 120, 364–374.
437   Kabelitz, T., Biniasch, O., Ammon, C., Nübel, U., Thiel, N., Janke, D., Swaminathan, S., Funk,
438   R., Münch, S., Rösler, U., Siller, P., Amon, B., Aarnink, A.J.A., Amon, T., 2021.
439   Particulate matter emissions during field application of poultry manure - The influence of
440   moisture content and treatment. Sci. Total Environ. 780.
441   Kearns, S.G., Bärlocher, F., 2008. Leaf surface roughness influences colonization success of
442   aquatic hyphomycete conidia. Fungal Ecol. 1, 13–18.
443   Kim, K., Jeon, J., Jung, H., Kim, T.K., Hong, J., Jeon, G.S., Kim, H.S., 2022. PM2.5 reduction
444   capacities and their relation to morphological and physiological traits in 13 landscaping tree
445   species. Urban For. Urban Green. 70, 127526.
446   Kim, S.-D., Kim, C.-H., Hwang, U.-H., 2008. A study on the particles density estimation in
447   Seoul metropolitan. J. Environ. Heal. Sci. 34, 131–136.
448   Kim, Y., Wellum, G., Mello, K., Strawhecker, K.E., Thoms, R., Giaya, A., Wyslouzil, B.E.,
449   2016. Effects of relative humidity and particle and surface properties on particle
450   resuspension rates. Aerosol Sci. Technol. 50, 339–352.
451   Kończak, B., Cempa, M., Pierzchała, Ł., Deska, M., 2020. Assessment of the ability of roadside
452   vegetation to remove particulate matter from the urban air. Environ. Pollut. 268, 115465.
453   Kottapalli, K., Novosselov, I. V., 2021. Aerodynamic resuspension and contact removal of
454   energetic particles from smooth, rough, and fibrous surfaces. Talanta 231, 122356.
455   Krauter, P., Biermann, A., 2007. Reaerosolization of fluidized spores in ventilation systems.
456   Appl. Environ. Microbiol. 73, 2165–2172.
457   Krogstad, P.Å., Antonia, R.A., 1999. Surface roughness effects in turbulent boundary layers.
458   Exp. Fluids 27, 450–460.
459   Li, Y., Zhang, X., Li, M., Yin, S., Zhang, Z., Zhang, T., Meng, H., Gong, J., Zhang, W., 2022.
460   Particle resuspension from leaf surfaces: Effect of species, leaf traits and wind speed. Urban
461   For. Urban Green. 77, 127740.
462   Liang, D., Ma, C., Wang, Yun qi, Wang, Yu jie, Chen-xi, Z., 2016. Quantifying PM2.5 capture
463   capability of greening trees based on leaf factors analyzing. Environ. Sci. Pollut. Res. 23,
464   21176–21186.
465   Loosmore, G.A., 2003. Evaluation and development of models for resuspension of aerosols at
466   short times after deposition. Atmos. Environ. 37, 639–647.
467   MacDonald, M., Chan, L., Chung, D., Hutchins, N., Ooi, A., 2016. Turbulent flow over
468   transitionally rough surfaces with varying roughness densities. J. Fluid Mech. 804, 130–
469   161.
470   Maffia, J., Aarnink, A.J.A., Ploegaert, J.P.M., Dinuccio, E., Balsari, P., Ellen, H.H., 2021.
471   Assessing particulate matter (PM10) emissions from outdoor runs in laying hen houses by
472   integrating wind tunnel and lab-scale measurements. Biosyst. Eng. 210, 1–12.

473   Martuzevicius, D., Kliucininkas, L., Prasauskas, T., Krugly, E., Kauneliene, V., Strandberg, B.,
474   2011. Resuspension of particulate matter and PAHs from street dust. Atmos. Environ. 45,
475   310–317.
476   McDonald, A.G., Bealey, W.J., Fowler, D., Dragosits, U., Skiba, U., Smith, R.I., Donovan, R.G.,
477   Brett, H.E., Hewitt, C.N., Nemitz, E., 2007. Quantifying the effect of urban tree planting on
478   concentrations and depositions of PM10 in two UK conurbations. Atmos. Environ. 41,
479   8455–8467.
480   McPherson, E.G., Scott, K.I., Simpson, J.R., 1998. Estimating cost effectiveness of residential
481   yard trees for improving air quality in Sacramento, California, using existing models.
482   Atmos. Environ. 32, 75–84.
483   Memon, R.A., Leung, D.Y.C., Liu, C.H., 2010. Effects of building aspect ratio and wind speed
484   on air temperatures in urban-like street canyons. Build. Environ. 45, 176–188.
485   Mori, J., Fini, A., Galimberti, M., Ginepro, M., Burchi, G., Massa, D., Ferrini, F., 2018. Air
486   pollution deposition on a roadside vegetation barrier in a Mediterranean environment:
487   Combined effect of evergreen shrub species and planting density. Sci. Total Environ. 643,
488   725–737.
489   Münch, S., Papke, N., Thiel, N., Nübel, U., Siller, P., Roesler, U., Biniasch, O., Funk, R., Amon,
490   T., 2020. Effects of farmyard manure application on dust emissions from arable soils.
491   Atmos. Pollut. Res. 11, 1610–1624.
492   Nasr, B., Ahmadi, G., Ferro, A.R., Dhaniyala, S., 2019. Overview of mechanistic particle
493   resuspension models : comparison with compilation of experimental data. J. Adhes. Sci.
494   Technol. 33, 2631–2660.
495   Nasr, B., Ahmadi, G., Ferro, A.R., Dhaniyala, S., 2020. A model for particle removal from
496   surfaces with large-scale roughness in turbulent flows. Aerosol Sci. Technol. 54, 291–303.
497   Nicholson, K.W., 1993. Wind tunnel experiments on the resuspension of particulate material.
498   Atmos. Environ. Part A, Gen. Top. 27, 181–188.
499   Ould-dada, Z., Baghini, N.M., 2001. Resuspension of small particles from tree surfaces 35,
500   3799–3809.
501   Qian, J., Ferro, A.R., 2008. Resuspension of dust particles in a chamber and associated
502   environmental factors. Aerosol Sci. Technol. 42, 566–578.
503   Qian, J., Ferro, A.R., Fowler, K.R., 2008. Estimating the resuspension rate and residence time of
504   indoor particles. J. Air Waste Manag. Assoc. 58, 502–516.
505   Qian, J., Peccia, J., Ferro, A.R., 2014. Walking-induced particle resuspension in indoor
506   environments. Atmos. Environ. 89, 464–481.
507   Romzaykina, O.N., Vasenev, V.I., Paltseva, A., Kuzyakov, Y. V., Neaman, A., Dovletyarova,
508   E.A., 2021. Assessing and mapping urban soils as geochemical barriers for contamination
509   by heavy metal(loid)s in Moscow megapolis. J. Environ. Qual. 50, 22–37.
510   Ryu, J., Kim, J.J., Byeon, H., Go, T., Lee, S.J., 2019. Removal of fine particulate matter (PM2.5)
511   via atmospheric humidity caused by evapotranspiration. Environ. Pollut. 245, 253–259.
512   Saleh, A., 1993. Soil roughness measurement: Chain method. J. Soil Water Conserv. 48, 527 LP
513   – 529.
514   Salizzoni, P., Soulhac, L., Mejean, P., Perkins, R.J., 2008. Influence of a two-scale surface
515   roughness on a neutral turbulent boundary layer. Boundary-Layer Meteorol. 127, 97–110.
516   Schneider, C.A., Rasband, W.S., Eliceiri, K.W., 2012. NIH Image to ImageJ: 25 years of image
517   analysis. Nat. Methods 9, 671–675.

518   Shi, J., Zhang, G., An, H., Yin, W., Xia, X., 2017. Quantifying the particulate matter
519   accumulation on leaf surfaces of urban plants in Beijing, China. Atmos. Pollut. Res. 8, 836–
520   842.
521   Sigal, A., Danberg, J.E., 1990. New correlation of roughness density effect on the turbulent
522   boundary layer. AIAA J. 28, 554–556.
523   Speak, A.F., Rothwell, J.J., Lindley, S.J., Smith, C.L., 2012. Urban particulate pollution
524   reduction by four species of green roof vegetation in a UK city. Atmos. Environ. 61, 283–
525   293.
526   Thomsen, L.M., Baartman, J.E.M., Barneveld, R.J., Starkloff, T., Stolte, J., 2015. Soil surface
527   roughness: Comparing old and new measuring methods and application in a soil erosion
528   model. Soil 1, 399–410.
529   Volino, R.J., Schultz, M.P., Flack, K.A., 2009. Turbulence structure in a boundary layer with
530   two-dimensional roughness. J. Fluid Mech. 635, 75–101.
531   Wang, H., Shi, H., Wang, Y., 2015. Effects of weather, time, and pollution level on the amount
532   of particulate matter deposited on leaves of Ligustrum lucidum. Sci. World J. 2015, 9–11.
533   Wang, Y., Zhao, Y., Yao, J., 2019. Large eddy simulation of particle deposition and
534   resuspension in turbulent duct flows. Adv. Powder Technol. 30, 656–671.
535   Wróblewska, K., Jeong, B.R., 2021. Effectiveness of plants and green infrastructure utilization in
536   ambient particulate matter removal. Environ. Sci. Eur. 33.
537   Wu, Y.L., Davidson, C.I., Russell, A.G., 1992. Controlled wind tunnel experiments for particle
538   bounceoff and resuspension. Aerosol Sci. Technol. 17, 245–262.
539   Xu, X., Xia, J., Gao, Y., Zheng, W., 2020. Additional focus on particulate matter wash-off events
540   from leaves is required: A review of studies of urban plants used to reduce airborne
541   particulate matter pollution. Urban For. Urban Green. 48, 126559.
542   Yin, S., Lyu, J., Zhang, X., Han, Y., Zhu, Y., Sun, N., Sun, W., Liu, C., 2020. Coagulation effect
543   of aero submicron particles on plant leaves: Measuring methods and potential mechanisms.
544   Environ. Pollut. 257, 113611.
545   Yoo, S.Y., Kim, T., Ham, S., Choi, S., Park, C.R., 2020. Importance of urban green at reduction
546   of particulate matters in Sihwa Industrial Complex, Korea. Sustain. 12.
547   Zhang, W., Wang, B., Niu, X., 2017. Relationship between leaf surface characteristics and
548   particle capturing capacities of different tree species in Beijing. Forests 8, 1–12.
549   Zhang, X., Lyu, J., Han, Y., Sun, N., Sun, W., Li, J., Liu, C., Yin, S., 2020. Effects of the leaf
550   functional traits of coniferous and broadleaved trees in subtropical monsoon regions on
551   PM2.5 dry deposition velocities. Environ. Pollut. 265, 114845.
552   Zhang, Z., Gong, J., Li, Y., Zhang, W., Zhang, T., Meng, H., Liu, X., 2022. Analysis of the
553   influencing factors of atmospheric particulate matter accumulation on coniferous species:
554   measurement methods, pollution level, and leaf traits. Environ. Sci. Pollut. Res.
555   Zhao, X., Yan, H., Liu, M., Kang, L., Yu, J., Yang, R., 2019. Relationship between PM2.5
556   adsorption and leaf surface morphology in ten urban tree species in Shenyang, China.
557   Energy Sources, Part A Recover. Util. Environ. Eff. 41, 1029–1039.
558   Zheng, G., Li, P., 2019. Resuspension of settled atmospheric particulate matter on plant leaves
559   determined by wind and leaf surface characteristics. Environ. Sci. Pollut. Res. 26, 19606–
560   19614.
561

Figure 1

Isometric views of the experimental settings and progress used in this study.

(a) the wind tunnel, (b) the test chamber with wind tunnel.
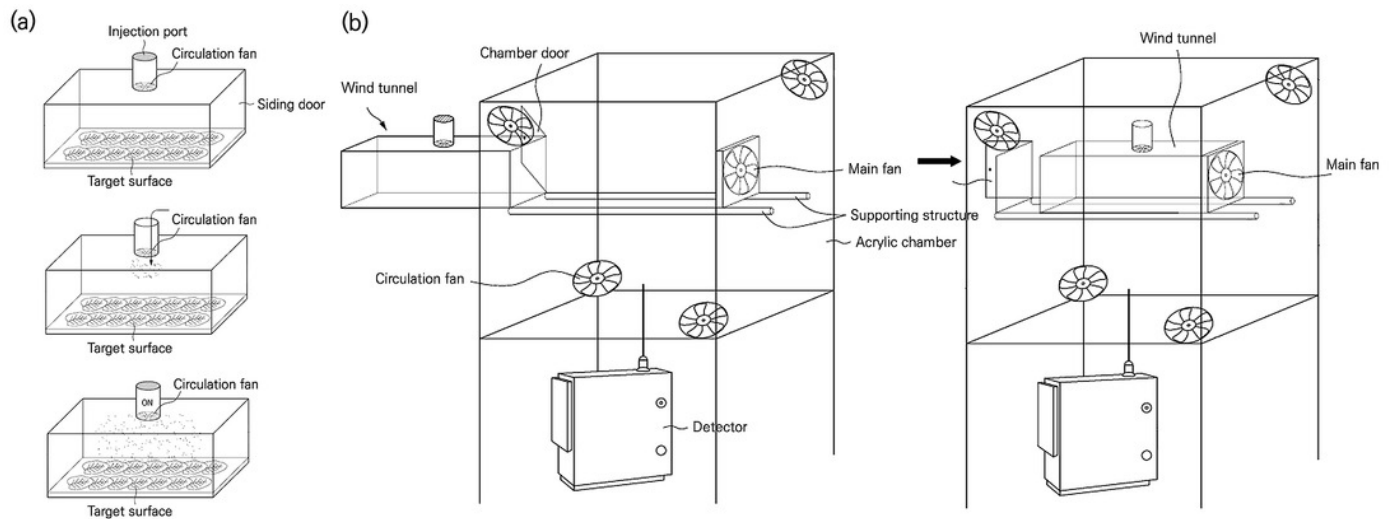
Figure 2

Photograph of surfaces simulated in this study, whose frame was made of 3 mm thick fomex for easy transport.

(A) Sand surface. (B) Coniferous litter layer on the sand surface. (C) Broadleaved litter layer on the sand surface.

Figure 3

Raw data pattern detected by EDM164.

The x-axis was time (s) and the y-axis was PM concentration($\mu g \cdot m^{-3}$). The main fan was operated for 10 min(vertical dashed line on the left), and the concentration converged to zero after about 30 min(vertical dashed line on the right).
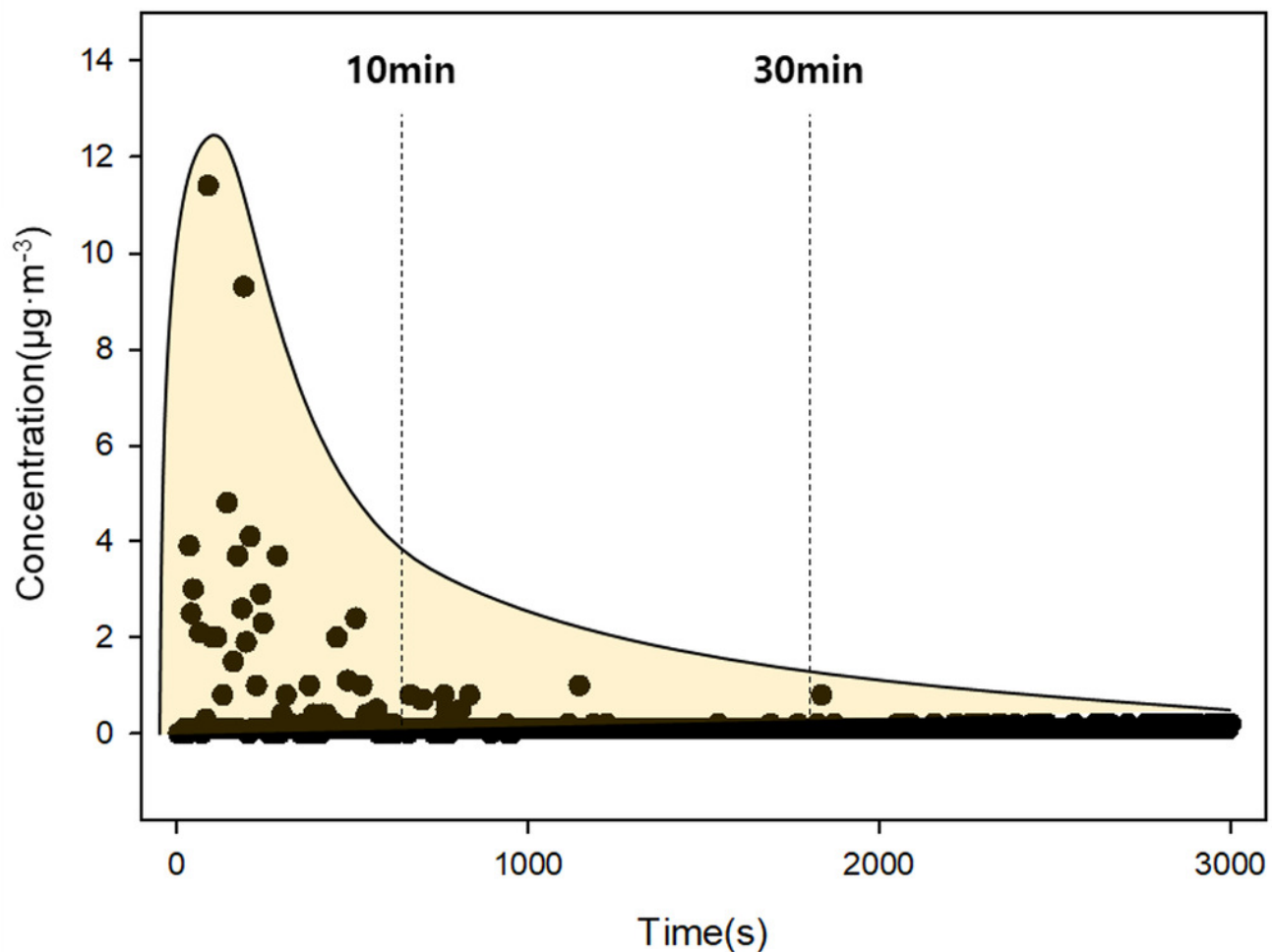
Figure 4

The process of verifying the experimental chamber design was shown in pictures over time (A–D).

The blue arrow indicates the direction of the wind from the main fan on the right. The black arrow indicates the flow in the chamber caused by the main flow. The flow in the chamber was determined by observing the water vapor from dry ice. It was verified that flow was formed only through the outlet at the bottom of the chamber (E), and the door was completely sealed by rubber (F).
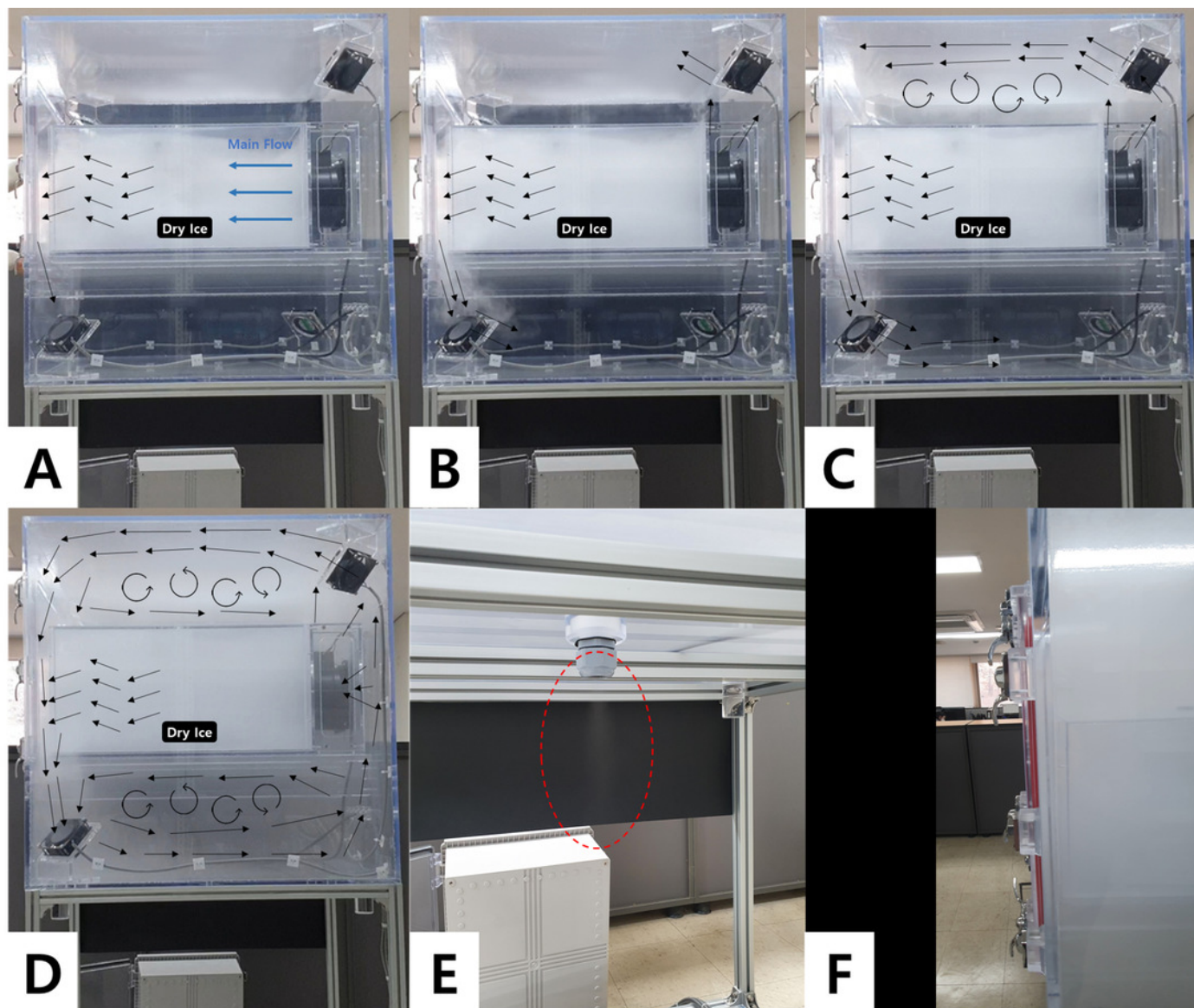
Figure 5

Surface roughness represented by *Cr* index by surface type (p<0.001).
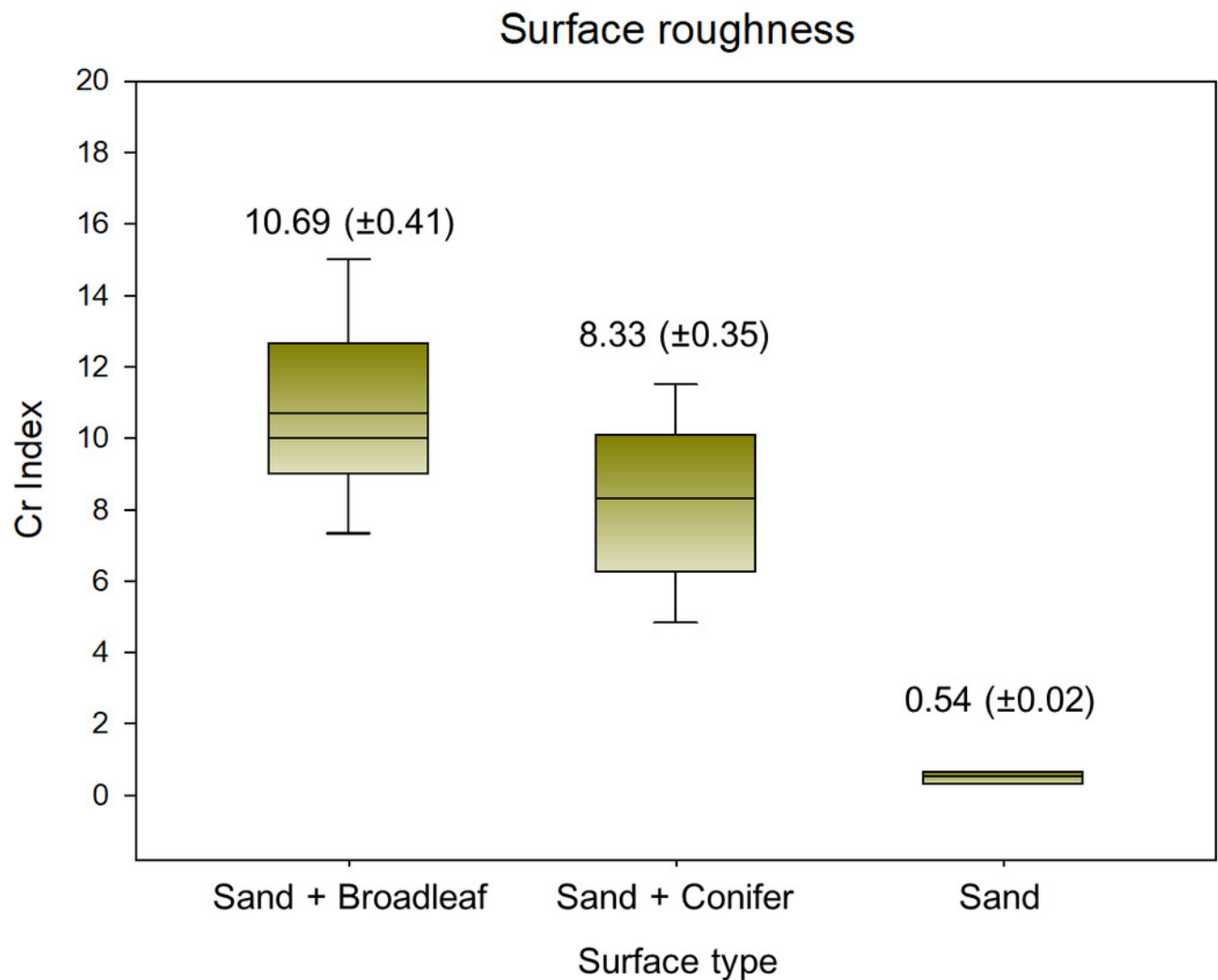
Figure 6

Total particulate matter resuspension rate by surface type (p<0.05).
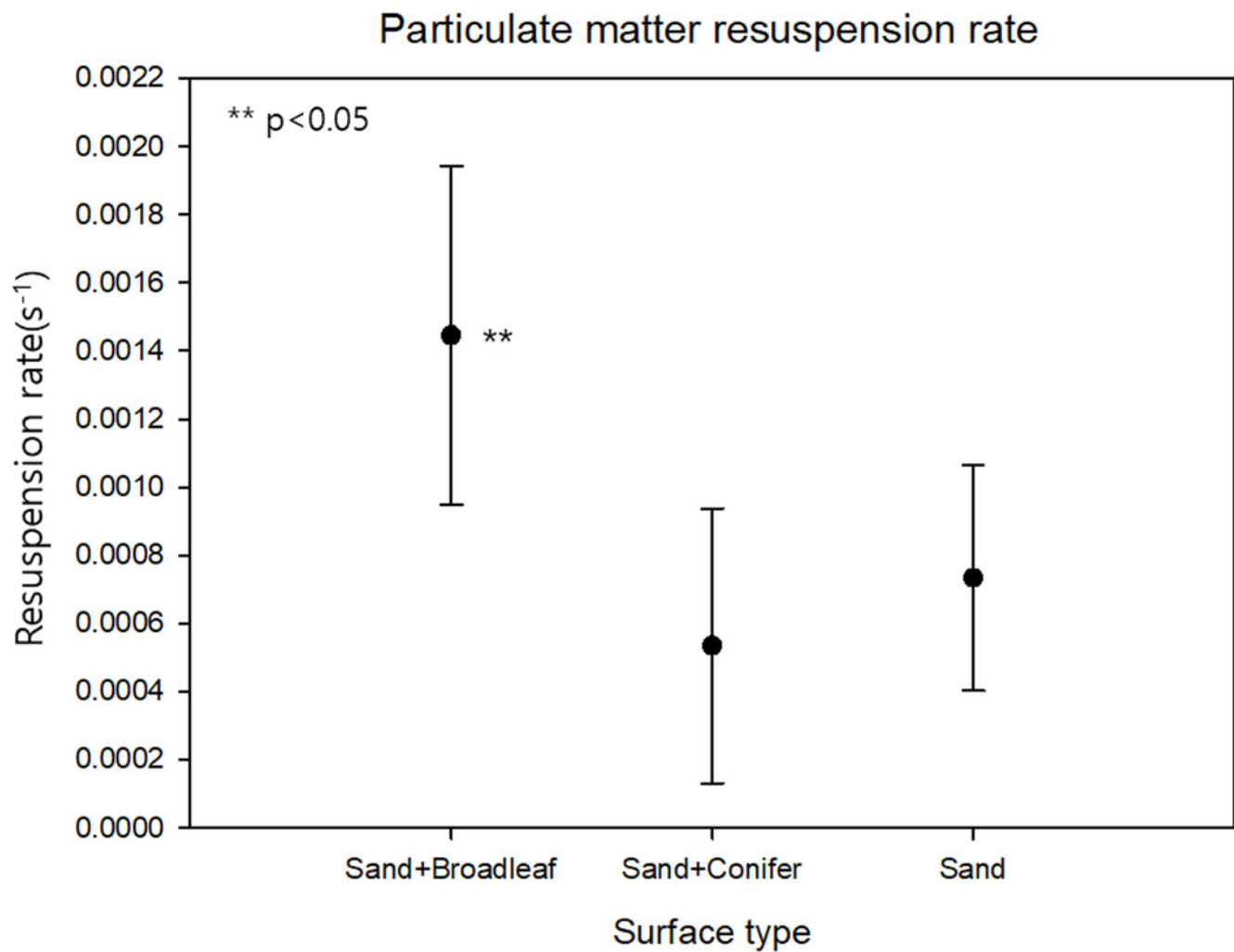
Figure 7

Relationship between surface roughness density and PM resuspension rate.

The solid line on the right shows a positive correlation on the millimeter scale (current study).
The dashed line on the left shows a negative correlation on the micrometer scale (existing
studies). Correlation coefficient (r) and equation are described in the upper-right.
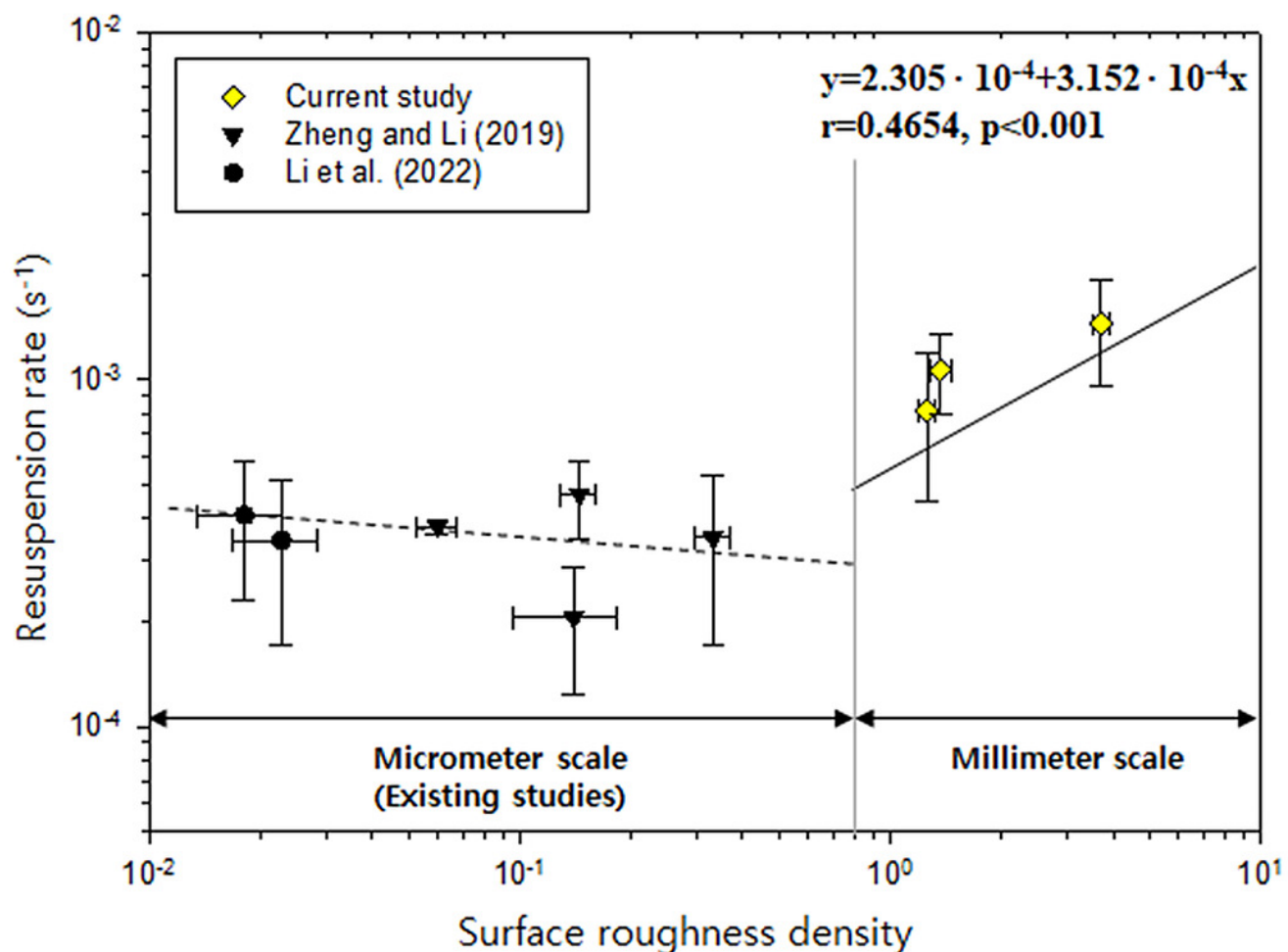
Figure 8

The number of resuspended PM.

(A) PM$_1$, (B) PM$_{1-10}$. The yellow boxes emphasize the appearance of difference between resuspended PM and initial PM sample.
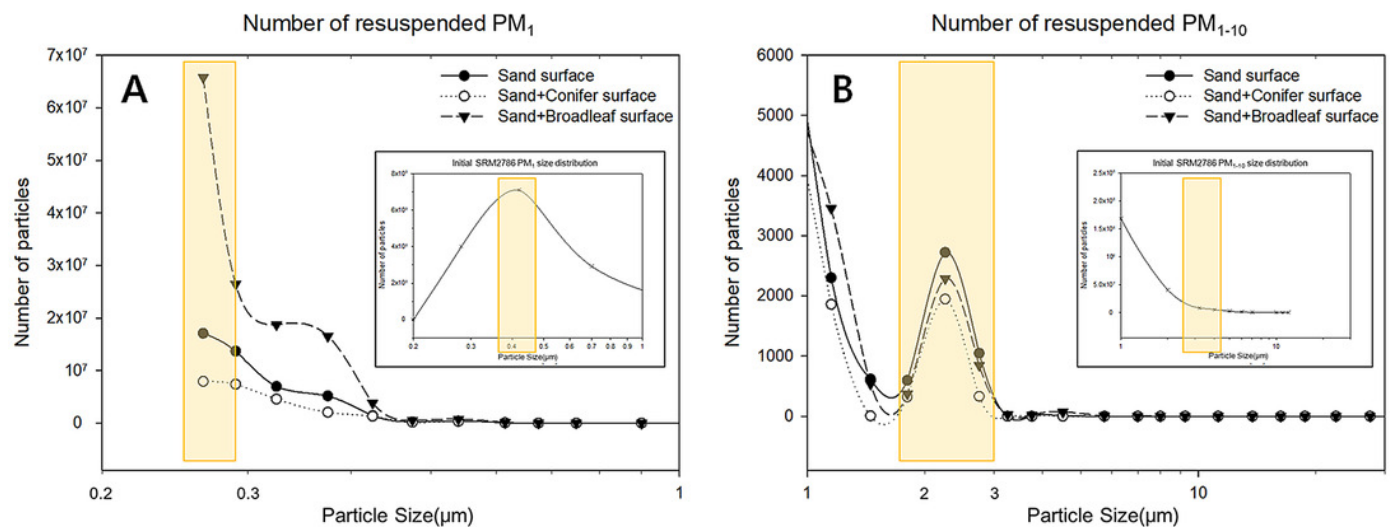
Technical specification data of EDM164.

Parameter	Specification
Particle size range	0.25–32 μm (31 size channels)
Particle number	0–3,000,000 particles·L^{-1}
Dust mass	0–100,000 μg·m^{-3} (unit: 0.1 μg·m^{-3})
Reproducibility	> 97% of total measuring range
Accuracy	87.3%*
Optical cell	Diode laser 660 nm
Time resolution	6 s, maximum 60 min
Sample flow rate	1.2 L·min^{-1}, ± 3% constant due to self-regulation
Rinsing air	0.4 L·min^{-1}, protection of laser optics, reference air for self-test
Sampling inlet	Heated, constant above ambient temperature
Temperature range	- 20–60°C (-4–140°F)
RH range	< 95%, non-condensing

1   TRANSPORTABLE AIR QUALITY MONITORING STATION EDM 164 Technical data (Grimm, 2021)

2   *EDM164 Performance Certificate (Certificate Korean Conformity Lab., 2019)

Particle size distribution information of NIST SRM No. 2786 sample.

	Size (μm)
Mean particle diameter, d(0.5)	2.8
Particle diameter, d(0.1)	0.91
Particle diameter, d(0.9)	6.9
Volume weighted mean	3.6

1   Certificate of Analysis Standard Reference Material® 2786 (NIST, 2021)